VIBRATION AND STRAIN SIGNAL ACQUISITION FOR NUMERICAL SIMULATION OF A COFFEE HARVESTER

Carlos Ademir da Silva
Federal University of Lavras (UFLA), Postgraduate program in Agricultural Engineering, Campus, ZIP Code 37,200-000, Lavras, MG, Brazil

Alexandre Assis Rezende Santos
Federal University of Lavras (UFLA), Postgraduate program in Systems Engineering and Automation, Campus, ZIP Code 37,200-000, Lavras, MG, Brazil

Leomar Santos Marques
Federal University of Lavras (UFLA), Postgraduate program in Agricultural Engineering, Campus, ZIP Code 37,200-000, Lavras, MG, Brazil
Corresponding author: leomar.marques@engenharia.ufjf.br

Ednilton Tavares de Andrade
Federal University of Lavras (UFLA), Postgraduate program in Agricultural Engineering, Campus, ZIP Code 37,200-000, Lavras, MG, Brazil

Ricardo Rodrigues Magalhães
Federal University of Lavras (UFLA), Postgraduate program in Agricultural Engineering, Campus, ZIP Code 37,200-000, Lavras, MG, Brazil

Abstract: Coffee harvesters utilize vibration systems to dislodge coffee beans. The vibration system is usually coupled to the end of an axis (rod cylinder). This cylinder can fail in the field, which usually occurs by means of cracks close to its flange in the region that promotes vibration. Numerical simulations are typically used to predict strains and stresses based on vibration signals in machines in general. This work acquired the vibration and strain signals of a coffee harvester rod cylinder prototype and compared the results using finite element analysis. To this end, a rod cylinder system was prototyped on a reduced scale (1:3) to recreate frequency and strain data, which were used for numerical simulation comparisons. The results showed that the predicted von Mises stress in the analyzed zone was 16.47 MPa (below the material yield strength, 250 MPa) based on a frequency of 14.2 Hz applied to the rod cylinder. This confirmed that cracks found in rod cylinders in the field are not generated by high stresses, as reported in the literature. The results demonstrated the potential of finite element analysis for strain and stress prediction when applied to agricultural machine components.

Index terms: Finite element method; coffee harvesting; strain and stress prediction.

Received: July 27, 2022 - Accepted: October 26, 2022

INTRODUCTION

In the past, coffee was harvested manually or semi mechanically. With current improvements in agricultural machinery, modern coffee harvesters can be self-propelled or tractor driven. The agricultural machinery sector has brought together industries dedicated to the manufacture of self-propelled machines such as coffee harvesters. According to the National Association of Automotive Vehicle Manufacturers (ANFAVEA, 2020), 4072 grain harvesters were sold in Brazil in 2020, even during pandemic scenarios. This represents a potential market for the development of new products. The agricultural and road machinery sector exported almost US$ 1.5 billion from January to October 2020 and generated more than 19000 direct jobs in Brazil.

Coffee harvester machines work at a frequency range of vibrations to achieve the resonance frequency of coffee beans, thus promoting their dislodgement (Tinoco et al., 2014; Coelho et al., 2015; Tinoco and Peña, 2018a; Tinoco and Peña, 2018b). Tractor-driven coffee harvesters generalized are designed with

two rod cylinders, which are responsible for promoting the vibration of coffee plant branches during harvesting. The vibration frequency has a regulation range that comprises the coffee bean detachment force. As a result of these machine vibrations, failures can occur in the rod cylinder in the field.

Numerical methods have been employed in vibration analysis, and one of most commonly used is the finite element method (Zienkiewicz et al., 2005). Commercial finite element software uses equations in vibratory system responses, providing displacement, velocity and acceleration, and other data (Rao, 2008). In agricultural engineering, finite element solutions have been applied in agricultural mechanization, product processing and soil mechanics (Velloso et al., 2018).

The method shows promise being constantly applied in the coffee harvest, among them Velloso et al. (2020) evaluated the dynamic behavior of the coffee tree and Carvalho et al. (2016) propose an evaluation of the mechanical behavior of the coffee structure by modeling through finite element analysis.

To predict coffee harvester failures in the field, some studies have considered numerical simulations (Silva et al., 2014; Silva et al., 2018; Souza et al., 2018). In addition, other studies have been developed to predict failures in machines and components (Qi et al., 2019; Yarenet al., 2019; Qinglin et al., 2019; Shlyannikov and Ishtyryakov, 2019; Silva et al., 2020), including the welded joints of low-alloy steels (Berdnikova et al., 2019) and silos (Cao et al., 2019).

Studies involving the design and simulation of coffee harvesters are increasing; Moreira et al. (2016) proposed a preliminary design of a coffee harvester. This justifies further research in the area for considering simulations for agricultural machines. Based on this need, this work aimed to predict the strain in a coffee harvester vibrating cylinder by using numerical simulations.

Preliminary Concepts of Vibration And Deformation Signal Background

All rotating machines have a certain level of vibration that cannot always be characterized as a mechanical defect. Currently, many agricultural machines operate with vibration systems, including mechanized coffee harvesters. In this case, vibratory alternating machine behavior can be an indication of a defect due to warping, misalignment or imbalance, causing wear and reducing the useful life of the equipment. Frequency signal analysis normally involves a Fourier transform to be applied to a signal that develops in time, transposing it to a frequency domain. This transformation makes it possible to identify the different frequency components of a signal as accurate information regarding the individual amplitude values and the possible lags between them. The Fourier transform for continuous signals that develop from -∞ to + ∞, in complex form, is given by Equation 1.

$$X(\omega) - \int_{-\infty}^{+\infty} x(t) e^{-iax} dt \quad (1)$$

where X (ω) is a complex function of frequency in which the Fourier transform of x (t) is absolutely integrated.

The visualization of the frequency spectrum is important for the analysis of vibration in rotating equipment. This view makes it possible to associate the frequency components and their amplitude with the mechanical components, thus providing support for the diagnosis of the causes of vibration. Through computational methods, the discrete Fourier transform was developed, which works with a signal in the time domain in a discrete form. The agility of the calculations enabled the development of portable signal analyzers equipped with a fast Fourier transform (FFT). Using this technique, signals from samples in the time domain can be converted to a frequency spectrum composed of different values.

The observation of the vibration level over time allows us to identify when the intensity of vibration, the repetition rate of a given phenomenon, the smoothness or the speed changes. The occurrence of changes in the original form of the signal may indicate the beginning of a failure in the equipment.

One of the most commonly used sensors used to measure the deformation of a material is the strain gauge. It is produced from a material

with known electrical resistance, as shown in Equation 2.

$$R = \rho \frac{L}{A} \quad (2)$$

where R is the electrical resistance, ρ is the resistivity of the material, L is the length of the filament and A is the cross-sectional area of the sensor filament.

Generally, strain gauges are added to an electronic circuit using Wheatstone bridges. The connection of a Wheatstone bridge with the sensors converts the electrical resistance into an electrical voltage signal, which can be measured according to the force applied to the material.

The electrical voltage is calculated by means of Ohm's law from the difference in the electrical resistance (Equation 2) before and after load application. Knowing the gauge factor (GF), which is provided by the sensor manufacturer, it is possible to convert collected values into strain values, as shown in Equation 3.

$$\varepsilon = \frac{\Delta V}{GF} \quad (3)$$

where is the strain, ΔV is the difference in electrical voltage before and after load application and GF is the gauge factor.

Once strain gauges are positioned at 45° according to Figure 1, it is possible to calculate the principal strains (1, 2) from Equation 4 (OMEGA, 2020).

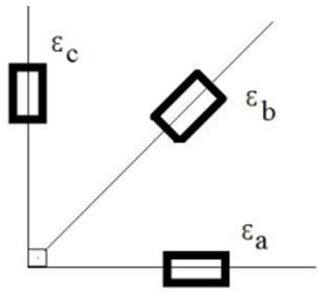

Figure 1: Three strain gauges (a, b, c) positioned at 45°.

$$\varepsilon_{1,2} = \frac{1}{2}\left(\varepsilon_a + \varepsilon_c \pm \sqrt{\left(\varepsilon_a - \varepsilon_c\right)^2 + \left(2\varepsilon_b - \varepsilon_1 - \varepsilon_3\right)^2}\right) \quad (4)$$

where e_1 is the maximum principal strain, e_2 is the minimum principal strain, and e_a, e_b and e_c are strains measured by the sensors (Figure 1).

MATERIAL AND METHODS

A flowchart for the steps performed in this work is shown in Figure 2.

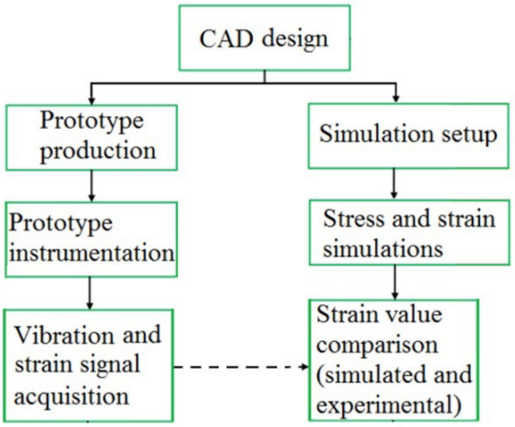

Figure 2: Flowchart of the steps performed in this work.

CAD design

Based on a real tractor-propelled coffee harvester, a reduced-scale prototype project (1:3) was developed according to Figure 3.

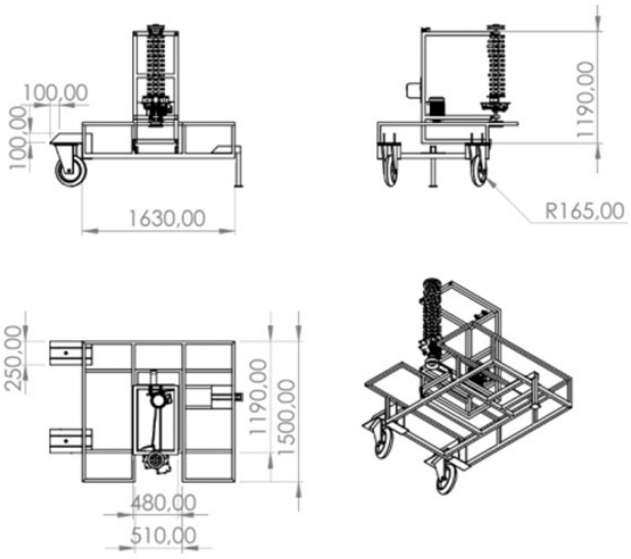

Figure 3: Coffee harvester machine prototype CAD model.

Prototype production and instrumentation

A mechanical system was coupled to the end of a rod cylinder (Figure 4). This mechanical system was positioned between two SAE 1020 steel plates (upper and lower) 750 mm in length, 400 mm in width and 15 mm in thickness.

Each plate was drilled in the center, at a diameter of 260 mm for the major flange and at a diameter of 160 mm for the minor flange, adapting a mechanical system in the rod cylinder by means of 20 screws (diameter of 15 mm each). Equidistant from these two central holes, there were four other holes with a diameter of 55 mm that fixed the axes of two 25 kg counterweights. At the four ends of the two plates, 4 spacer screws, each 200 mm long and 30 mm in diameter, were attached. These four screws worked with four nuts on each to promote the separation of the two plates. A frequency inverter coupled to a 1 CV electric engine was used to promote the vibration in the rod cylinder (Figure 5).

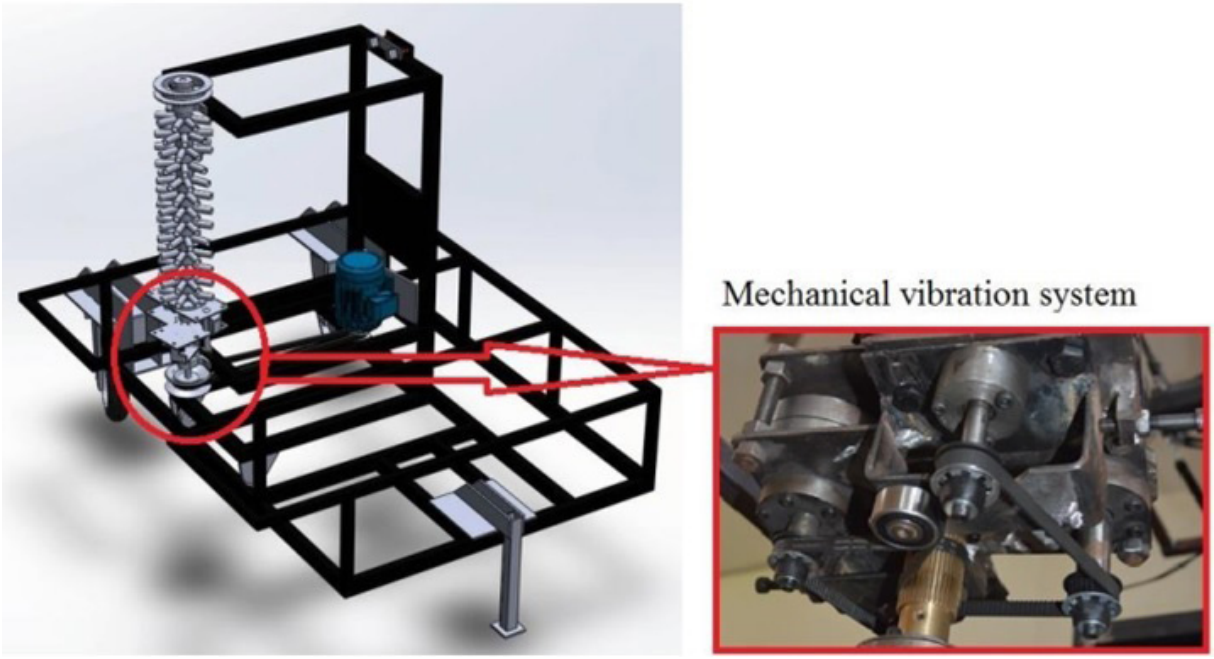

Figure 4: Mechanical vibration system.

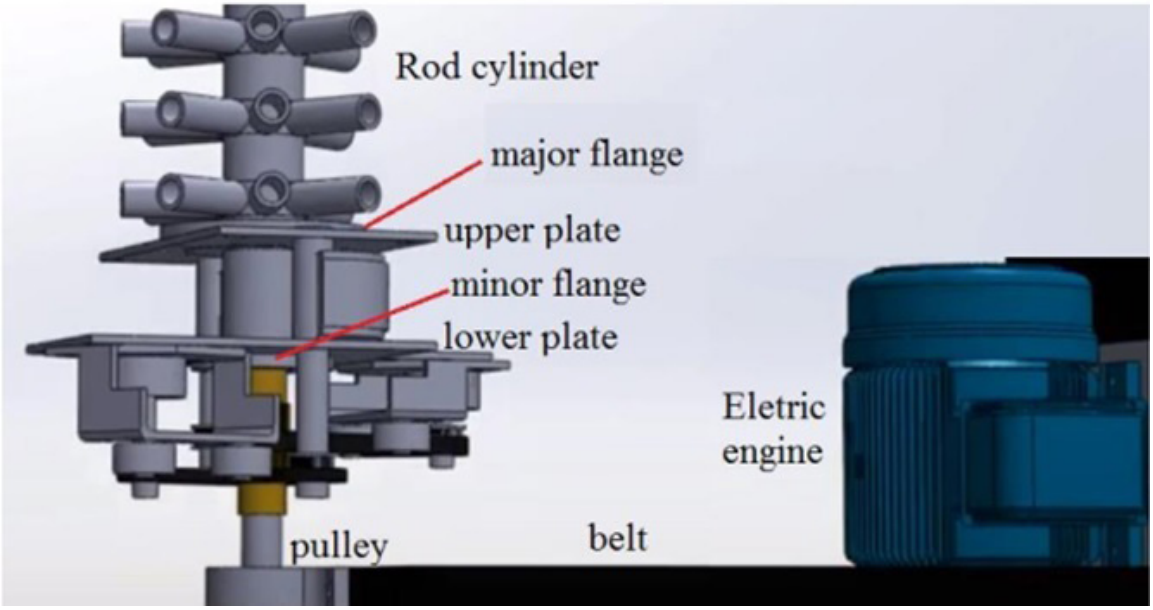

Figure 5: Mechanical system details.

By using a frequency inverter, it was possible to regulate the three working frequencies of the harvester in the field (12.5 Hz, 14.2 Hz and 15.8 Hz) as proposed by Ferreira Jr. et al. (2016b). First, it was necessary to regulate the frequencies in the inverter to the rod cylinder.

For acceleration and strain signal acquisition, National Instruments NI 9237 and NI 9949 were used. The software used to communicate with the hardware was LabView version 16.0f2. An accelerometer and strain gauges positioned at 45° were installed in the rod cylinder according to Figure 6.

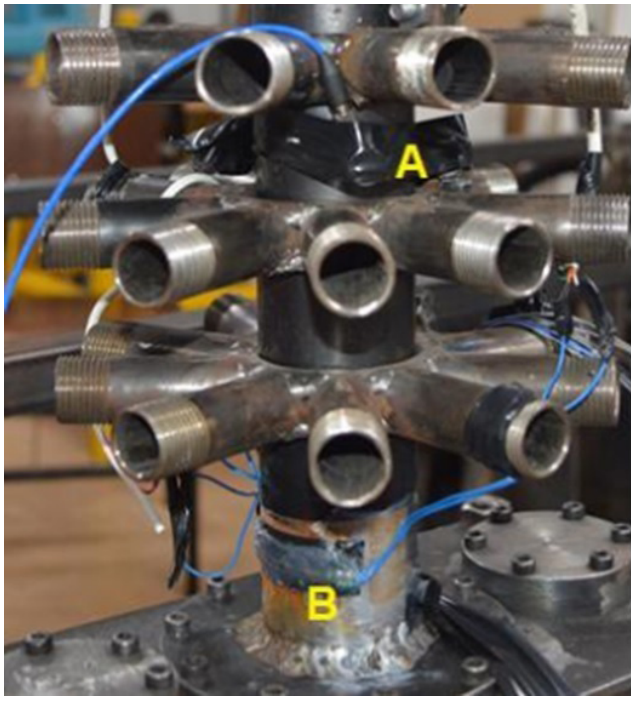

Figure 6: Accelerometer (A) and strain gauge (B) positions.

Numerical simulations

For the coffee harvester vibrating cylinder simulations, the commercial software Ansys version 14.5 was used. The model was based on a stainless-steel SAE 1010 tube with a 10 mm wall thickness, 130 mm outside diameter and 2.33 m length. To simplify the vibrating cylinder model (computational cost savings) the accommodation geometries of the rods and flange holes were removed. For this, the influence of removed geometries was verified in terms of mechanical stresses. It was noted that simulated stress values were not changed for both situations (cylinder with and without flange holes and rod accommodation geometries).

Structural steel material was used for the rod cylinder simulations (same material as the real piece) and its main mechanical properties are shown in Table 1.

Table 1: Rod cylinder material mechanical properties.

Mechanical property	Value
Density	7850 kg m^{-3}
Tensile/Compressive Yield Strength	2.5e^{+8} Pa
Tensile Ultimate Strength	4.6 e^{+8} Pa
Poisson's Ratio	0.3
Young's Modulus	2 e^{+11} Pa

For the initial simulation conditions, three different remote displacement positions in the rod cylinder were considered, which represented regions with restricted movements by means of bearings and the contact between the machine and plants, as shown in Figure 7. As suggested by Ferreira Jr. et al. (2016a), a torque of 64.33 Nm (maximum value from three studies) was applied to the brake disk region, which corresponded to a load of 2570 N, also detailed in Figure 7.

To simulate the influence of the coffee plants being contacted by the rods, a small value of 0.00025 rad of remote displacement in the Z rotation direction was assumed. Moreover, alternating rotation about the Z axis (Θ) was applied to the rod cylinder major flange (Figure 8) to reproduce the real cylinder movement, according to Equation 5.

$$\theta = A \sin(\omega t) \quad (5)$$

where Θ is the rotation angle about the Z axis, A is the amplitude, w is the constant angular velocity and t is the simulation time.

As proposed by Souza et al. (2018), A = 0.002 m was used. Time values were used according to the frequency imposed on the cylinder (12.5 Hz corresponded to 0.08 s, 14.2 Hz corresponded to 0.07 s and 15,8 Hz corresponded to 0.06 s).

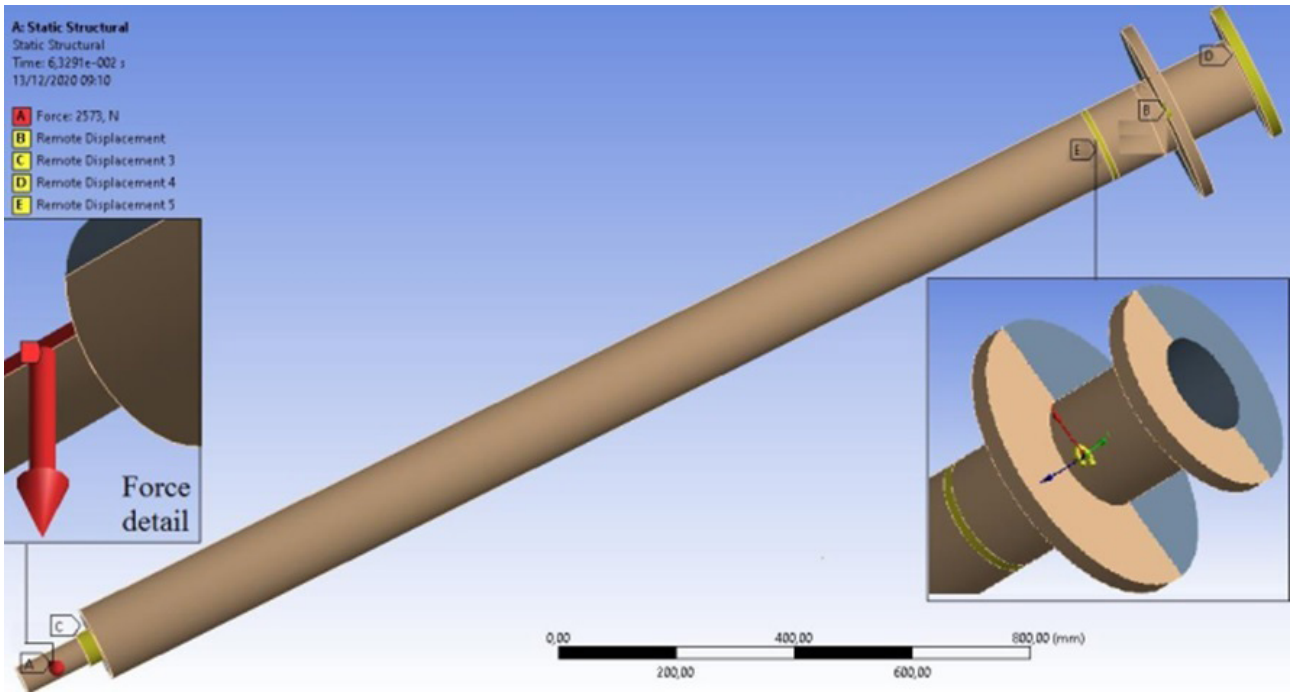

Figure 7: Initial setup for the simulations.

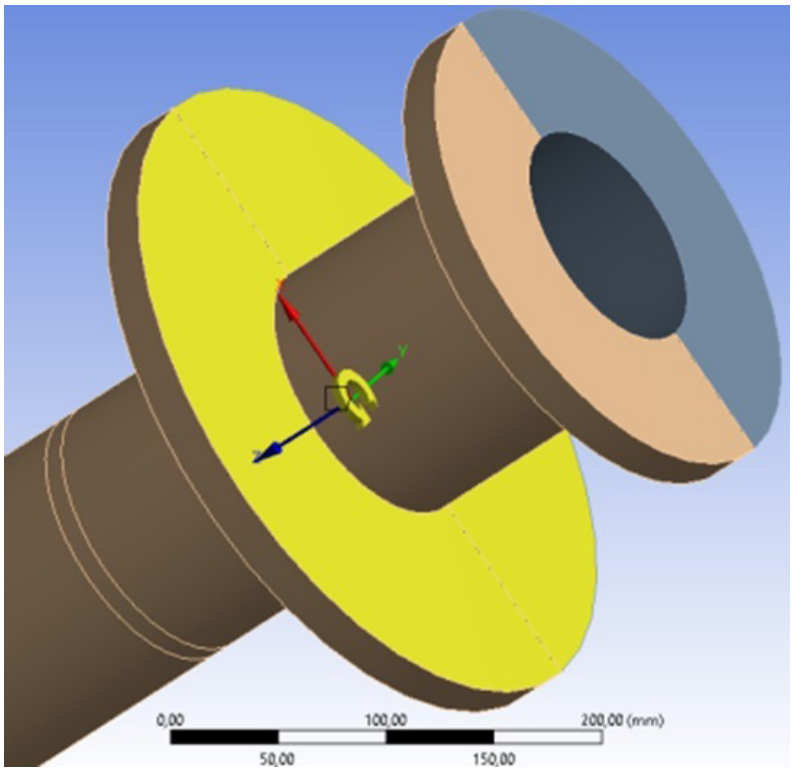

Figure 8: Alternating rotation angle about Z axis.

Transient structural analysis was considered for the simulations, and it was necessary to generate the mesh (discretized model) from the vibrating cylinder geometry. After mesh convergence analysis, the model generated 19498 nodes and 9622 second-order tetrahedron elements. Considering the regions where strain gauges were positioned in the real part, a local refined model was generated for the finite element model (Figure 9).

To track strain evolution during the simulations, a strain probe was added to the

same region where the strain gauges were positioned, as shown in Figure 10.

RESULTS AND DISCUSSION

Mesh convergence analysis

For the mesh convergence analysis, the von Mises stress at a specific region from the rod cylinder geometry was monitored. The mesh convergence results (Figure 11) showed a von Mises stress stabilization tendency before 20000 nodes.

Accelerometer signals

Three replicas for each tested frequency (15.8 Hz, 14.2 Hz and 12.5 Hz) were provided, as shown in Table 2.

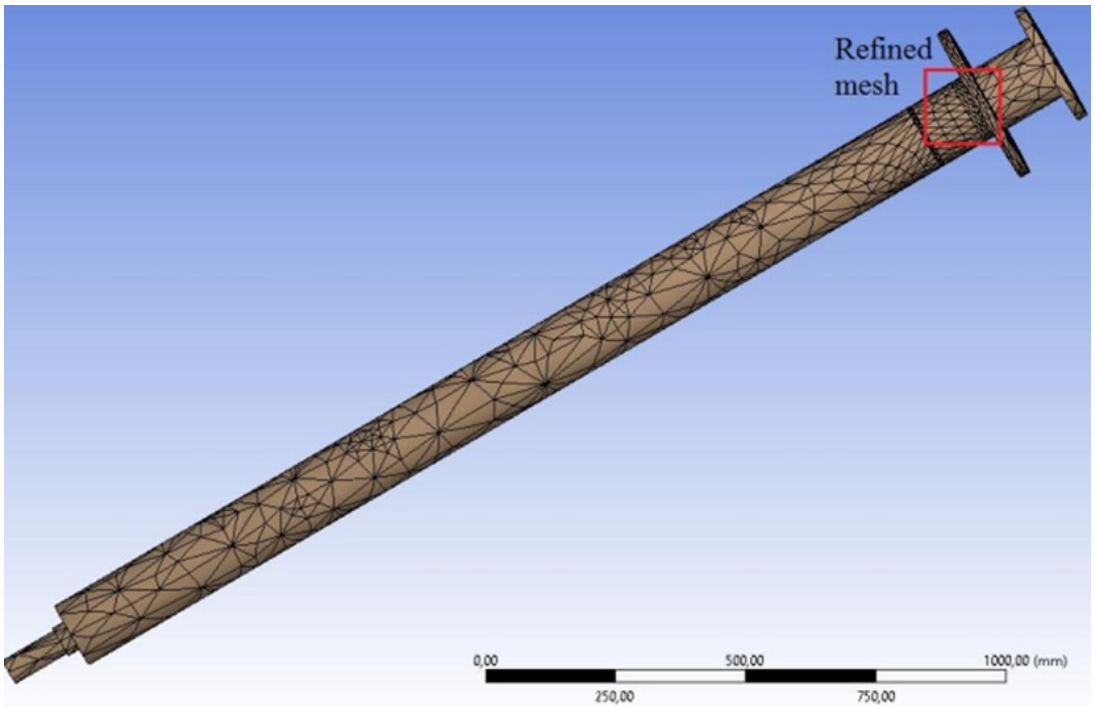

Figure 9: Rod cylinder finite element model.

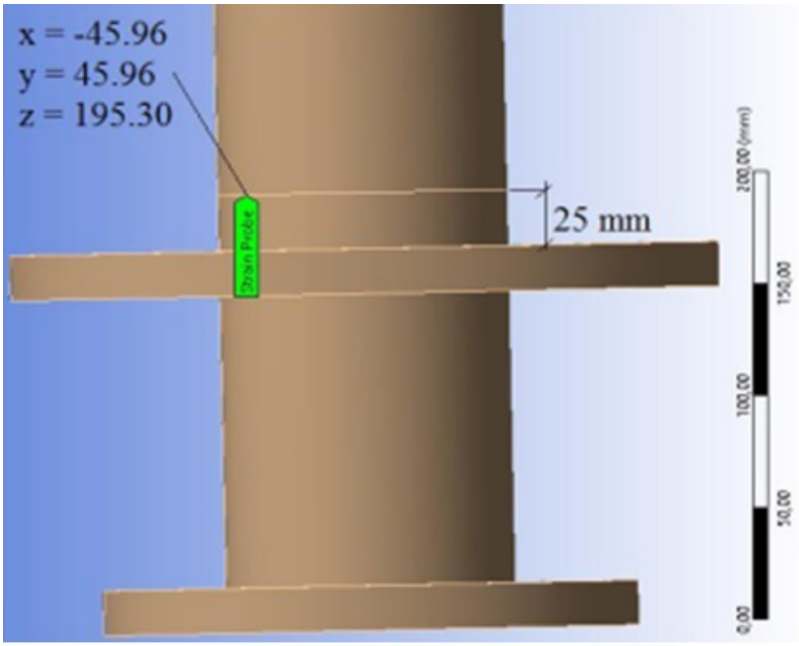

Figure 10: Rod cylinder strain probe.

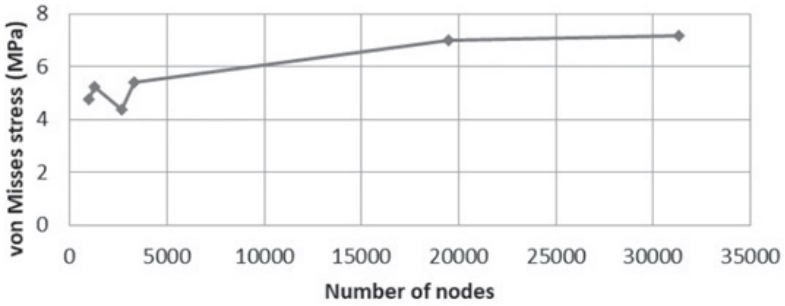

Figure 11: Mesh convergence analysis results.

Table 2: Rod cylinder material mechanical properties.

Frequency inverter (Hz)	Replica 1 (Hz)	Replica 2 (Hz)	Replica 3 (Hz)	Average (Hz)
15.8	15.5	15.7	15.9	15.7
14.2	14.3	14.2	14.2	14.2
12.5	12.3	12.6	12.5	12.5

An FFT vibration response diagram considering the frequency of 15.8 Hz applied to the inverter for Replica 1 (Table 2) is represented by Figure 12.

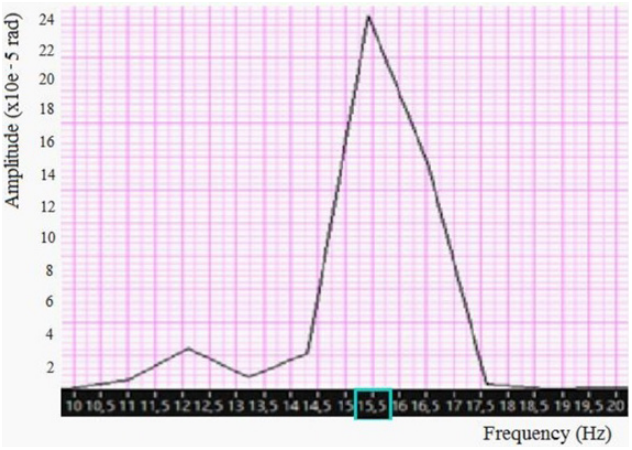

Figure 12: FFT vibration response for the Replica 1 (15.8 Hz).

Based on the accelerometer signal response, it was possible to reproduce vibrations of a real coffee harvest machine for the proposed prototype.

Strain signals and simulations

Five replicas were performed for each measured strain value according to the applied frequency. The mean strain values and the calculated maximum principal strains (Equation 4) are presented in Table 3.

Table 3: Rod cylinder material mechanical properties.

Measured strain	Frequency (Hz)		
	12.5	14.2	15.8
e_a	0.00003	0.00004	0.00005
e_b	0.00005	0.00006	0.00007
e_c	0.00002	0.00003	0.00004
Maximum principal strain	0.00005	0.00006	0.00007

The simulated strain values for 12.5 Hz, 14.2 Hz and 15.8 Hz were $6.22e^{-5}$, $6.23e^{-5}$ and $6.24e^{-5}$, respectively. A comparison between the experimental data (Table 3) and simulated results for the maximum principal strain is presented in Figure 13.

It can be seen in the chart (Figure 13) that the closest value between the experimental and simulated strain results is at the frequency of 14.2 Hz (difference of 2.94%), note that from the frequencies suggested by other works, the frequency at which this study was able to achieve the closest approximation between the two methodologies was 14.2 Hz, it is believed that this fact was due to the stabilization of frequencies and the expected difference between real and numerical, therefore recommends, so it is recommended to use this frequency value as a reference for further numerical simulations. Based on this result, Figure 14 shows the evolution of the strain over the simulation time, and Figure 15 presents the von Mises stress simulation, both considering a frequency of 14.2 Hz in the probe coordinate.

Figure 15 shows that the maximum von Mises stress at the probe was 16.47 MPa, and the maximum von Mises stress value found in the rod cylinder was 21.22 MPa. Based on the

simulated results, it can be affirmed that the component has a low possibility of presenting failure as a result of the determined von Mises stress much below the material yield strength (250 MPa, Table 1). This suggests that rod cylinder cracks found in the field are generated by faulty welding or manufacturing defects, as reported by Silva et al. (2020).

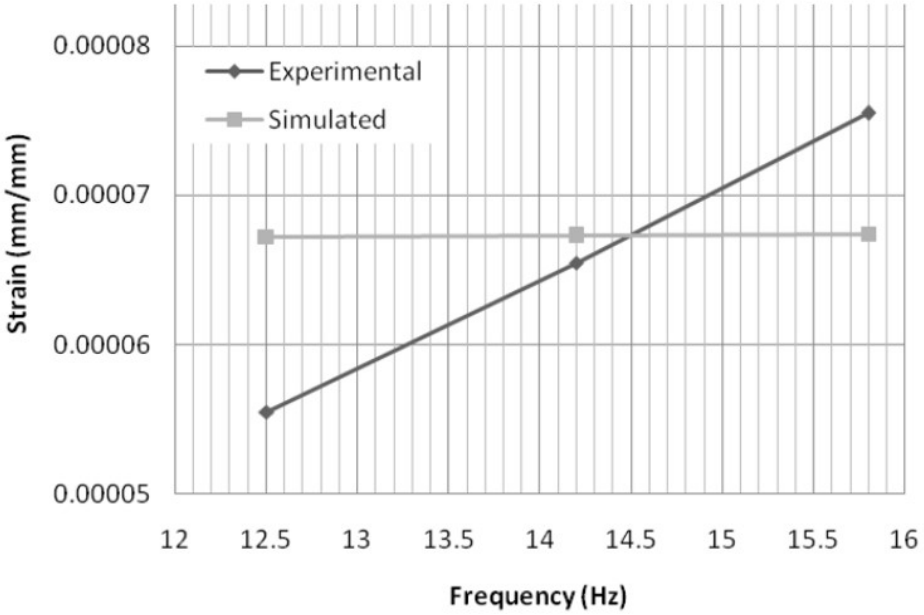

Figure 13: Experimental vs. simulated strain results.

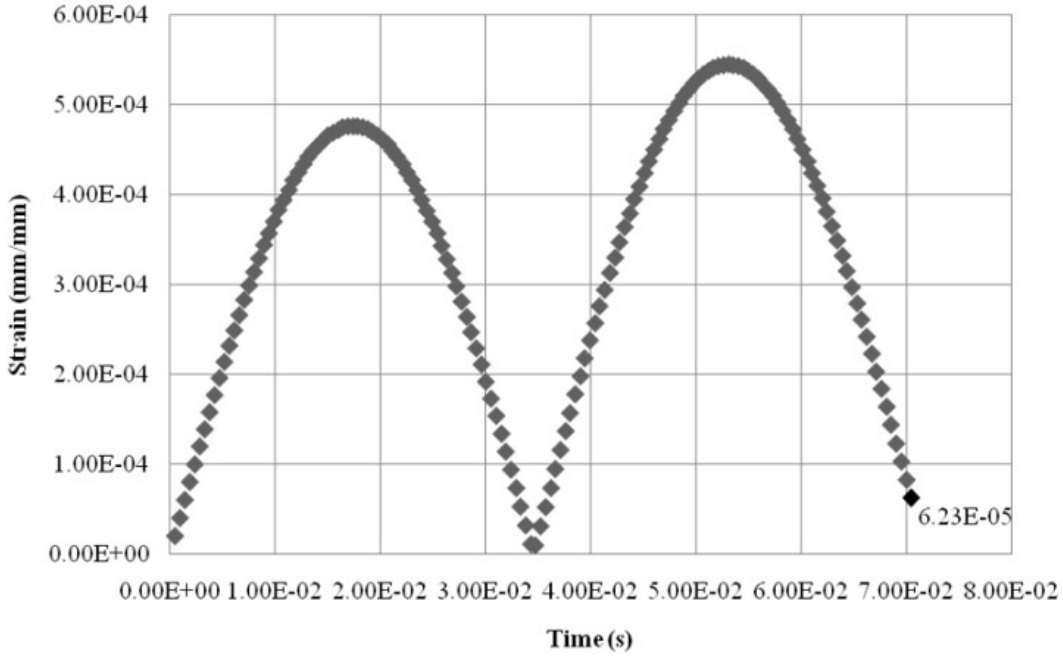

Figure 14: Strain evolution along the simulation time.

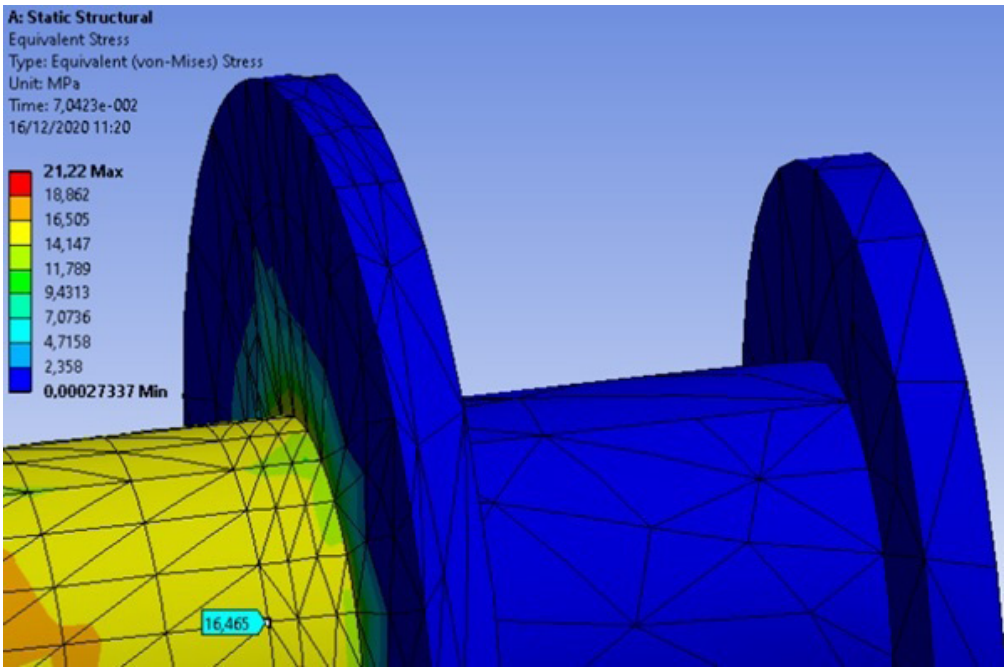

Figure 15: Simulated von Mises stress.

CONCLUSIONS

This work performed vibration and strain signal acquisition from a coffee harvester rod cylinder. The part was modeled and prototyped at a reduced scale (1:3) to promote vibration/strain data and run numerical simulations. The results showed a difference of 2.94% between the experimental and simulated strain values, considering a frequency of 14.2 Hz. For the same frequency, the predicted von Mises stress was 16.47 MPa (below the material yield strength, 250 MPa) in the analyzed region of the rod cylinder. This confirmed that cracks found in real rod cylinders are not generated by high stress, as reported in the literature. The results also demonstrated the potential of finite element analysis for strain and stress prediction when applied to agricultural machine components. For future works, it is proposed to run new simulations considering thermal effects from the welding process.

ACKNOWLEDGMENTS

The authors would like to thank University of Lavras (UFLA) for this research support.

REFERENCES

ANFAVEA. **Association of Automotive Vehicle Manufacturers**. In: <http://www.anfavea.com.br/estatisticas-copiar.html/>, Accessed: 7 nov, 2020.

BERDNIKOVA, O. et al. Effect of the structure on the mechanical properties and cracking resistance of welded joints of low-alloyed high-strength steels. **Procedia Structural Integrity**, 16:89-96, 2019.

CAO, Q. et al. Nonlinear buckling of cylindrical steel silos with fabrication cracks. **Powder Technology**, 353:219–229, 2019.

CARVALHO, E. A.; MAGALHÃES R. R.; SANTOS, F. L. Geometric modeling of a coffee plant for displacements prediction. **Computers and Electronics in Agriculture**, 123:57-63, 2016.

COELHO, A.L.F.; SANTOS, F.L.; PINTO, F.A.C.; QUEIROZ, D.M. Determination of geometric, physical and mechanical properties of coffee fruit-stem-branch system. **Revista Brasileira de Engenharia Agrícola e Ambiental**, 19(3), 286-292, 2015.

FERREIRA JR. L. G.; SILVA, F. M.; FERREIRA, D. D.; SALES, R. S. Recommendation for mechanical harvesting of coffee based on vibration behavior settings rods harvesters. **Ciencia Rural**, 46(2), 273-278, 2016a.

FERREIRA JR., L.G.; SILVA, F. M.; FERREIRA, D. D. Displacement Tracking of Harvester Rods of a Coffee Harvester**. IEEE Latin America Transactions**, 14(12):4674- 4680, 2016b.

MOREIRA, R. M. G. et al. Preliminary design of a coffee harvester. **Semina: Ciências Agrárias**, 37(5):2933-2946, 2016.

OMEGA. **Strain gauge installation: How to position strain gauges to monitor, bending, axial, shear, and torsional loads**. In: <https://www.omega.co.uk/techref/pdf/Strain-gauge-application-info/how-to-position-strain-gauges.pdf>, Accessed: 14 dec, 2020.

QI, S.; CAI, L. X.; BAO, C.; CHEN, H.; SHI, K. K.; WU, H. L. Analytical theory for fatigue crack propagation rates of mixed-mode I–II cracks and its application. **International Journal of Fatigue**, 119:150-159, 2019.

QINGLIN, L. et al. Crack propagation behavior in white etching layer on rail steel surface. **Engineering Failure Analysis**, 104:816-829, 2019.

RAO, S. **Mechanical Vibrations**. (5th ed.), Pearson PrenticeHall, 2010, 1084 p.

SHLYANNIKOV, V.N.; ISHTYRYAKOV, I.S. Crack growth rate and lifetime prediction for aviation gas turbine engine compressor disk based on nonlinear fracture mechanics parameters. **Theoretical and Applied Fracture Mechanics**, 103:102313, 2019.

SILVA, C. A. DA; CAMPOS, A. A. R.; MAGALHÃES, R.; ANDRADE, E. T. DE; VOLPATO, C. E. S.; MARQUES, L. S. Experimental analysis in a stell cylinder of a coffee harvest for failure diagnosis. **ForScience**, 8(2):e00632, 2020.

SILVA, E. P.; SILVA, F. M.; MAGALHÃES, R. R. Application of finite elements method for structural analysis in a coffee harvester. **Engineering**, 6:138-147, 2014.

SILVA, E. P.; SILVA, F. M.; ANDRADE, E. T.; MAGALHAES, R. R. Structural static and modal frequency simulations in a coffee harvester`s chassis. **Revista Brasileira de Engenharia Agricola e Ambiental**, 22:511-515, 2018.

SOUZA, V. H. S.; DIAS, G. L.; SANTOS, A. A. R.; COSTA, A. L. G.; SANTOS, F. L.; MAGALHAES, R. R. Evaluation of the interaction between a harvester rod and a coffee branch based on finite element analysis. **Computers and Electronics in Agriculture**, 150:476-483, 2018.

TINOCO, H. A.; PEÑA, F. M. Finite Element Analysis of Coffee arabica L. var. Colombia Fruits for Selective Detachment Using Forced Vibrations. **Vibration**, 1:207- 219, 2018b.

TINOCO, H. A.; PEÑA, F. M.. Harmonic stress analysis on Coffe aarábica L. var. Colombia fruits in order to stimulate the selective detachment: A finite element analysis. **Simulation**, 94(2):163-174, 2018a.

TINOCO, H. A.; OCAMPO, D. A.; PEÑA, F. M.; SANZ-URIBE, J. R. Finite element modal analysis of the fruit-peduncle of Coffeaarabica L. var. Colombia estimating its geometrical and mechanical properties. **Computers and Eletronics in Agriculture**, 108:17-27, 2014.

VELLOSO, N. S.; COSTA, A. L. G.; MAGALHÃES, R. R.; SANTOS, F. L.; ANDRADE, E. T. (2018). The Finite Element Method Applied to Agricultural Engineering: A Review. **Current Agriculture Research Journal**, 6(3):286-299, 2018.

VELLOSO, N. S., R. R., SANTOS, F. L, SANTOS, A. A. R. Modal properties of coffee plants via numerical simulation, **Computers and Electronics in Agriculture**, 175:105552, 2020.

YAREN, M. F. et al. Three-dimensional mode-I/III fatigue crack propagation: Computational modeling and experiments. **International Journal of Fatigue**, 121:124-134, 2019.

ZIENKIEWICZ, O. C.; TAYLOR, R. L.; ZHU, J. Z. **The finite element method: its basis and fundamentals**. Elsevier Butterworth-Heinemann, 2005, 733p.

DRUMOND, T. P.; MACIEL, D. N. GRECO, M. Dynamic analysis of a flare tower in off-shore platforms. **Theoretical and Applied Engineering**, 1(1):20-30, 2017.